Differential Lipid Binding of Truncation Mutants of *Galleria mellonella* Apolipophorin III

Matthias Dettloff,[‡] Marc Niere,[‡] Robert O. Ryan,[§] Robert Luty,[⊥] Cyril M. Kay,[⊥] Andreas Wiesner,[‡] and Paul M. M. Weers*[,§]

Institute of Biology/Zoology, Free University of Berlin, Königin-Luise-Strasse 1−3, D-14 195 Berlin, Germany, Lipid Biology in Health and Disease Research Group, Children's Hospital Oakland Research Institute, 5700 Martin Luther King Jr. Way, Oakland, California 94609, USA, Protein Engineering Network of Centres of Excellence (PENCE), Department of Biochemistry, University of Alberta, Edmonton, Alberta T6G 2S2, Canada

Received January 8, 2002; Revised Manuscript Received May 14, 2002

ABSTRACT: Apolipophorin III (apoLp-III) is a prototype exchangeable apolipoprotein that is amenable to structure−function studies. The protein folds as a bundle of five amphipathic α-helices and undergoes a dramatic conformational change upon lipid binding. Recently, we have shown that a truncation mutant of *Galleria mellonella* apoLp-III comprising helices 1−3 is stable in solution and able to bind to lipid surfaces [Dettloff, M., Weers, P. M. M., Niere, M., Kay, C. M., Ryan, R. O., and Wiesner, A. (2001) *Biochemistry 40*, 3150−3157]. To investigate the role of the C-terminal helices in apoLp-III structure and function, two additional 3-helix mutants were designed: a core fragment comprising helix (H) 2−4, and a C-terminal fragment (H3−5). Each truncation mutant retained the ability to associate spontaneously with dimyristoylphosphatidylcholine (DMPC) vesicles, transforming them into discoidal complexes. The rate of apolipoprotein-dependent DMPC vesicle transformation decreased in the order H1−3 > H2−4 > H3−5. Truncation of two helices led to a significant decrease in α-helical content in buffer in each case, from 86% (wild-type) to 50% (H1−3), 28% (H2−4), and 24% α-helical content (H3−5). On the other hand, trifluoroethanol or complexation with DMPC induced the truncation mutants to adopt a high α-helical structure similar to that of wild-type protein (84−100% α-helical structure). ApoLp-III(H1−3) and apoLp-III(H2−4), but not apoLp-III(H3−5), were able to prevent phospholipase-C-induced low density lipoprotein aggregation, indicating that interaction of the C-terminal fragment with spherical lipoprotein surfaces was impaired. As lipoprotein binding is significantly affected and DMPC transformation rates are relatively slow upon removal of N-terminal helices, the data indicate that structural elements necessary for lipid interaction reside in the N-terminal part of the protein.

Insect apolipophorin III (apoLp-III)[1] is an amphipathic, α-helical exchangeable apolipoprotein. It represents a model apolipoprotein for studies of fundamental aspects of apolipoprotein structure and function (*1*). Studies on the mechanistic and structural aspects of apoLp-III benefit our understanding of the molecular basis of lipid-related diseases that are linked to apolipoprotein function. As with mammalian exchangeable apolipoproteins, such as apolipoprotein (apo) E and apoA-I, apoLp-III reversibly binds to lipoprotein surfaces, facilitated by the presence of amphipathic α-helices (*2*). The protein is normally present in a water-soluble form and acquires a lipid bound state upon encountering an appropriate lipid surface. Three-dimensional structures have been reported for apoLp-III in the lipid-free state for two evolutionary divergent insect species that share low sequence homology: *Locusta migratoria*, solved by X-ray crystallography (*3*), and *Manduca sexta*, solved by NMR spectroscopy (*4*). These globular proteins consist of five amphipathic α-helices, organized in an antiparallel up-and-down topology. Hydrophobic faces of amphipathic α-helices orient toward the protein interior, while hydrophilic residues are exposed on the protein exterior ensuring protein solubility in aqueous environments. This molecular architecture has a striking resemblance with the four-helix bundle of the N-terminal domain of apoE (*5*), and may be a common folding pattern of apolipoproteins in their lipid-free state. Whereas high-resolution structural data of apoLp-III in the lipid-bound state are unavailable, a model has been proposed on the basis of the lipid-free structure (*3*). It was hypothesized that, upon lipid association, helix 1, 2, and 5 move apart from helix 3 and 4, exposing the hydrophobic faces of amphipathic α-helices allowing formation of a stable complex with lipid. Biophysical and functional data have provided experimental evidence that the protein unfurls upon association with lipid surfaces while maintaining its high α-helical character (*6*−*11*). Recently, an alternative model of apoLp-III lipid binding was postu-

[†] Supported by NIH (HL64159, to R.O.R.), Deutsche Forschungsgemeinschaft (WI 1612/1-2, to A.W.), Friedrich-Ebert-Stiftung (M.D.) and Sonnenfeld-Stiftung (M.N.).

* To whom correspondence should be addressed. Tel: 510-428-3885 x2965. Fax: 510-450-7910. E-mail: pweers@chori.org.

[‡] Free University of Berlin.

[§] Children's Hospital Oakland Research Institute.

[⊥] University of Alberta.

[1] Abbreviations: ANS, 8-anilinonaphthalene-1-sulfonate; apo, apolipoprotein; apoLp-III, apolipophorin III; CD, circular dichroism; DMPC, dimyristoylphosphatidylcholine; HDLp, high-density lipophorin; LDL, low-density lipoprotein; LDLp, low-density lipophorin; PL-C, phospholipase C; SDS−PAGE, sodium dodecyl sulfate−polyacrylamide gel electrophoresis; TFE, trifluorethanol.

10.1021/bi0200108 CCC: $22.00
Published on Web 06/22/2002

lated. Lipid-triggered helix relaxation, in which helix 1 and 5 separate from each other, is postulated to lead to exposure of the hydrophobic protein core, which is then able to interact directly with the lipid surface (*12*, *13*). At present, the precise orientation of helices in lipid associated apoLp-III remains unknown and is one of the main aims of future research.

The primary role of apoLp-III is to bind to lipid-enriched lipoprotein substrates thereby stabilizing the lipoprotein particle (*14*, *15*). Recently, apoLp-III from *Galleria mellonella* has been identified as an immune stimulating factor which has been linked to apoLp-III's lipid binding properties (*16*−*19*). *G. mellonella* apoLp-III is very similar to apoLp-III from *M. sexta*, sharing 69% sequence identity (*17*). In an earlier study, a truncated apoLp-III from *G. mellonella*, composed of the first three N-terminal helices was designed (*20*). This truncation mutant was able to bind to phospholipid vesicles and associate with a lipoprotein surface, indicating retention of its functions as an apolipoprotein. This led to questions about the role of the remaining helices in the intact protein. To evaluate the function of the C-terminal part of the protein, deletion mutants were constructed, each comprising three complete helices. Deletion of helices from the N-terminal and/or C-terminal end of the protein yielded a core and a C-terminal fragment, respectively. Biophysical and lipid binding studies of these mutant three-helix proteins provide evidence that, although the 3-helix mutants were able to interact with model phospholipid membranes, lipoprotein binding was impaired after removal of N-terminal helices.

MATERIALS AND METHODS

Mutagenesis. The nucleotide sequences encoding residues 32−129, and 70−163 of *G. mellonella* apoLp-III were amplified from a full-length cDNA template (*17*) with *Pfu* polymerase (Stratagene) as described (*20*). The following oligonucleotide primers were employed: 5′-CCG ACA CCA AGG AGT TCA ACA CCG-3′ and 5′-GCC GGA ATT CTT ACT CCT CCA GGT TGG CGC-3′ for apoLp-III(32−129); 5′-CCA AGG AGG CGC TGG AGC AGA CG-3′ and 5′-CGG AAT TCT TAC TGC TTG CTG GCG GCC TCG TG-3′ for apoLp-III(70−163). The amplification products were digested with *Eco*RI and ligated into the pET 22b+ vector (Novagen) via its *Msc*I and *Eco*RI-sites and transformed into *Escherichia coli* BL 21 (DE3) cells. DNA sequences were verified by cycle sequencing following evaluation with an automated DNA sequencer (Licor 4000L, MWG-Biotech).

Expression and Purification of Recombinant Proteins. Expression and purification of recombinant wild-type and truncation mutant apoLp-IIIs was carried out in a bacterial expression system as outlined previously (*20*). Sample purity was verified by analytical RP-HPLC and sodium dodecyl sulfate−polyacrylamide gel electrophoresis (SDS−PAGE) using 4−20% acrylamide gradient gels (*21*). Gels were stained with Coomassie Blue. The molecular mass of the truncation mutants was verified by electrospray mass spectrometry (VG quattro mass spectrometer, Fisons instruments, Manchester, UK). For calculation of protein concentrations, fringe counts of the truncation mutant samples were performed as described previously (*20*).

Circular Dichroism Spectroscopy and Fluorescence. Circular dichroism (CD) spectroscopy was performed using a JASCO J-720 spectropolarimeter calibrated with a 0.06% solution of ammonium d-camphor-10-sulfonate as described (*20*). Data were collected using J700 control driver version 1.20.00, J700 hardware manager version 1.10.00 and processed using J700 for windows standard analysis software version 1.20.00. Complexes of apoLp-III and DMPC were dialyzed against 50 mM sodium phosphate (pH 7.2) for 48 h. Prior to measuring ellipticity at 221 nm, samples treated with guanidine HCl were incubated for 24 h. CD spectra were analyzed for secondary structure by the Contin program of Provencher and Glöckner (*22*), using the 16 original reference proteins for the calculation of the α-helical content. Fluorescence studies were carried out using a Perkin-Elmer luminescence spectrometer (LS50B). Samples of 250 μM 8-anilinonaphthalene-1-sulfonate (ANS) and 50 μM protein were excited at 395 nm, and emission was monitored between 400 and 600 nm using a 5 nm slit width.

Analytical Ultracentrifugation. Sedimentation equilibrium experiments were carried out at 20 °C in a Beckman XL-I Analytical ultracentrifuge using Interference optics following the procedures described by Laue and Stafford (*23*). Aliquots of 100 μL sample solution were loaded into 6-sector CFE sample cells, allowing three concentrations of sample to be run simultaneously. Runs were performed at a minimum of two different speeds, and each speed was maintained until there was no significant difference in $r^2/2$ versus absorbance scans taken 2 h apart to ensure that equilibrium was achieved. The sedimentation equilibrium data was evaluated using the NONLIN program, which incorporates a nonlinear least-squares curve-fitting algorithm described by Johnson et al. (*24*). This program allows the analysis of both single and multiple data files. Data can be fit to either a single ideal species model or model containing up to four associating species, depending on which parameters are permitted to vary during the fitted routine. The protein's partial specific volume and the solvent density were estimated using the SEDNTERP program, which incorporates calculations detailed by Laue et al. (*25*).

Vesicle Transformation Assay. The rate of apoLp-III-induced transformation of phospholipid vesicles into protein−lipid complexes was monitored using a Perkin-Elmer Luminescence spectrometer (model LS 50B) as described (*11*). Excitation and emission wavelengths were set at 612 nm using a slit width of 3 nm. The temperature of the cuvette holder was maintained at 24 °C. Dimyristoylphosphatidylcholine (DMPC) vesicles were prepared by extrusion through a 200 nm filter as described (*11*). The vesicles (250 μg) were equilibrated in buffer (20 mM Tris HCl, pH 7.2, 150 mM NaCl, 0.02% EDTA) at 24 °C for 5 min in a 1-mL cuvette. Protein (250 μg) was added and mixed for 10 s, and the change in light scattering was monitored as a function of time.

Isolation and Characterization of ApoLp-III/DMPC Complexes. ApoLp-III (2 mg) was added to a dispersion of 5 mg of unilamellar DMPC vesicles, mixed, and incubated overnight at 24 °C. KBr (1.12 g) was added to the sample, and the volume was adjusted to 2.5 mL (density 1.27 g/mL). The samples were transferred to 5-mL Quick seal tubes, overlaid with 2.5 mL of 0.9% NaCl, and centrifuged at 65 000 rpm for 2 h at 4 °C in a VTi 65.2 rotor. Gradient fractions containing protein−lipid complexes were dialyzed against phosphate buffered saline (154 mM NaCl, 50 mM NaH_2PO_4, 50 mM Na_2HPO_4, 3.4 mM EDTA, pH 7.0). Aliquots of the com-

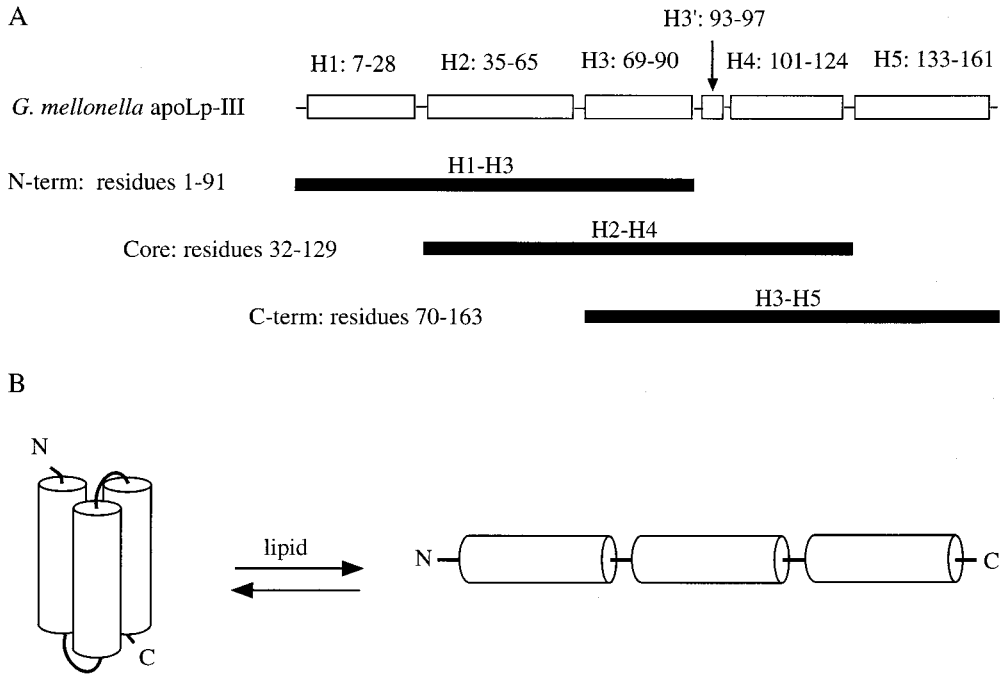

FIGURE 1: Design of apoLp-III truncation mutants. Panel A: The 3-helix proteins generated contained three consecutive α-helices. Shown are the residues and helices of each mutant apoLp-III. The helix boundaries of *G. mellonella* apoLp-III are based on sequence comparison with the closely related *M. sexta* apoLp-III for which high resolution structural data is available (*4*). The proteins share 69% amino acid identity (*28*). Panel B: Model of a 3-helix bundle apolipoprotein. This putative 3-helix protein bundle may be able to bury hydrophobic residues and maintain interhelical contacts and, in the presence of lipids, adopts an open conformation in which hydrophobic residues can interact directly with the lipid substrate.

plexes were subjected to native PAGE or were used for cross-linking with dimethyl suberimidate as described by (*7*, *20*). For electron microscopy analysis, the protein−lipid complexes were adsorbed to hydrophilized, carbon-coated grids. After rinsing the grids with buffer (10 mM Tris, 10 mM NaCl, 1.5 mM $MgCl_2$), they were negatively stained for 10 s with 2% sodium phosphotungstate, pH 7.0. Photographs were taken in a Philips EM 420 operated at 100 kV.

LDL Protection Assay. Binding of apoLp-III to lipoproteins was measured using the LDL protection assay (*26*, *27*). Human LDL (50 μg of protein) was incubated with 160 mU phospholipase C (PL-C, from *Bacillus cereus*, Sigma) in buffer (50 mM Tris HCl, pH 7.5, 150 mM NaCl and 2 mM $CaCl_2$) to generate apoLp-III binding sites on the lipoprotein surface. Incubations were carried out at 37 °C for 2 h in the presence or absence of indicated amounts of apoLp-III (200 μL final sample volume). The absorbance at 340 nm was measured spectrophotometrically at times indicated.

RESULTS

Design, Expression, and Purification of Truncation Mutants. The helix boundaries of *G. mellonella* apoLp-III were established on the basis of sequence alignment with the closely related *M. sexta* apoLp-III (*28*), whose high-resolution structure is available (*4*). The apoLp-III truncation mutants investigated were comprised of three consecutive helical segments (Figure 1). The presence of three helical segments would allow for potential interhelical contacts of the amphipathic α-helices, which may stabilize the protein tertiary structure. As depicted in Figure 1, the N-terminal fragment contained helices 1−3 (H1−3, residues 1−91), the core fragment contained helices 2−4 (H2−4, residues 32−129), and the C-terminal fragment contained helices 3−5 (H3−5, residues 70−163), thereby encompassing the entire apoLp-III amino acid sequence. Wild-type recombinant *G. mellonella* apoLp-III and the truncation mutants were overexpressed in *Escherichia coli* using the pET expression vector. Similar to the expression of wild-type apoLp-III and the N-terminal domain of human apoE3 (*17*, *29*−*31*), the truncation mutants escaped the bacteria with removal of the vector encoded signal peptide and accumulated into the culture medium. This feature greatly facilitated purification of the recombinant proteins as they were directly isolated from culture medium after removal of *E. coli* cells. While expression yields of apoLp-III(H1−3) and apoLp-III(H2−4) were approximately 40−70 mg of pure protein/L of culture medium, the yield of apoLp-III(H3−5) was substantially lower (10 mg/L). SDS−PAGE, RP-HPLC, and mass spectrometry verified the identity and purity of the designed apoLp-III truncation mutants (data not shown).

Phospholipid−apoLp-III Complex Formation. ApoLp-III binds spontaneously to dispersions of DMPC vesicles at their gel-to-liquid crystalline phase transition temperature, transforming them into discoidal protein−lipid complexes. The truncated mutants were tested for this detergent-like action by incubation with DMPC vesicles at the phospholipid transition temperature. Upon mixing of protein and lipid in a 1:1 mass ratio, wild-type apoLp-III induced clearance of a turbid DMPC suspension in about 2000 s, whereas in the absence of apolipoprotein the suspension remained turbid (Figure 2). Using the same mass ratio, apoLp-III(H1−3) and apoLp-III(H2−4) displayed much faster transformation rates compared to wild-type-apoLp-III, as indicated by the time required to achieve a 50% decrease in sample turbidity ($t_{1/2}$, Table 2). ApoLp-III(H3−5) showed transformation kinetics comparable to wild-type apoLp-III. However, apoLp-III(H3−5) displayed reduced transformation kinetics in comparison

Table 1: Biophysical Properties of ApoLp-III

	N-term H1−3	core H2−4	C-term H3−5	wild-type apoLp-III
α-helical content in buffer (%)[a]	50	28	24	86
α-helical content in TFE (%)	100	89	100	84
α-helical content with DMPC (%)	100	100	92	100
[guanidine HCl]$_{1/2}$ lipid-free (M)	0.4	n.d.	n.d.	0.3
[guanidine HCl]$_{1/2}$ DMPC (M)	3.0	2.25	2.0	3.5
Mw sequence[b]	10,104	10,743	10,623	18,075
Mw sedimentation equilibrium[c]	18,909	25,460	15,634	17,031
best fit model	mon-dim	mon-dim-tri	mon-dim	single species

[a] The percentage of α-helical content was calculated by the Contin program by Provencher and Glöckner (*22*) from the far UV CD spectra of the proteins. [Guanidine-HCl]$_{1/2}$ is the molar concentration of guanidine HCl required to cause a 50% decrease in ellipticity at 221 nm. [b] Molecular weight based on the amino acid sequence. [c] Molecular weight based on sedimentation equilibrium experiments.

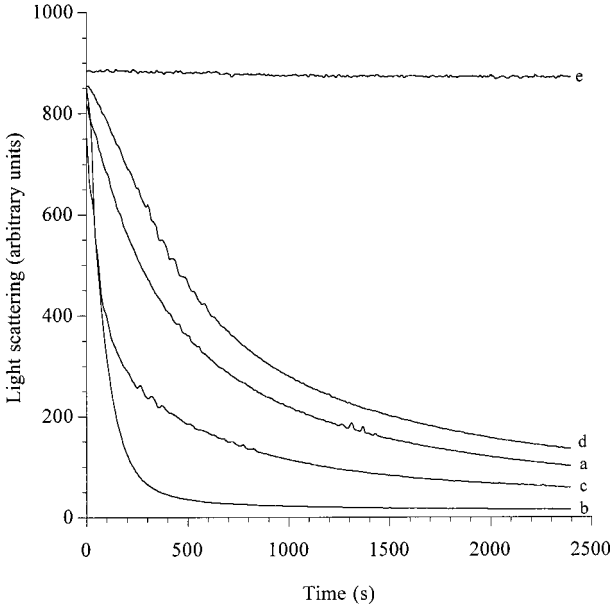

FIGURE 2: Apolipoprotein-induced phospholipid vesicle transformation. Mixtures of DMPC vesicles and apoLp-III were incubated at 24 °C using a phospholipid/protein mass ratio of 1:1. Transformation of the vesicles into the much smaller disks was monitored by 90° light scattering in a fluorescence spectrophotometer (excitation and emission wavelength set at 612 nm). Curve a: wild-type apoLp-III; curve b: apoLp-III(H1−3); curve c: apoLp-III(H2−4); curve d: apoLp-III(H3−5); curve e: vesicles in the absence of apolipoprotein.

Table 2: Properties of Discoidal Complexes of ApoLp-III/DMPC Complexes[a]

	N-term H1−3[b]	core H2−4	C-term H3−5	wild-type apoLp-III[b]
particle mass (kDa)	∼400	∼700	∼900	∼ 700
diameter (nm)	13.5 ± 2.4	17.6 ± 1.6	24.8 ± 3	17.7 ± 1.8
no. of apoLp-III molecules	7	6	9	5
DMPC $t_{1/2}$ (s)	80	90	450	425

[a] Particle masses were estimated from native PAGE; the diameters of the complexes were measured from electron micrographs. The number of apoLp-III molecules on a DMPC disk was determined by cross-linking studies; DMPC $t_{1/2}$ represents the time required for a 50% reduction of sample turbidity of a mixture of DMPC vesicles and apoLp-III, due to formation of discoidal complexes. [b] Obtained from Dettloff et al. (*20*).

to wild-type protein when equimolar protein amounts were used (data not shown).

Wild-type apoLp-III and the truncated mutants also disrupted negatively charged dimyristoylphosphatidylglycerol (DMPG) vesicles, a process that occurs at a much faster rate than with DMPC vesicles ($t_{1/2}$ of DMPG vesicles of wild-type apoLp-III equals 40 s). This is probably a result of strong electrostatic interactions between negatively charged phospholipid headgroups and positively charged amino acid side chains in apoLp-III. The lower DMPG packing density compared to DMPC as a result of charge repulsion of adjacent molecules may also facilitate protein binding and penetration. Transformation rates for the three truncation mutants were too fast to calculate as complete clearance was achieved during mixing (data not shown). These results demonstrate that the truncated mutants display the characteristic detergent-like action of exchangeable apolipoproteins, and form phospholipid−protein complexes. The lipid−protein complexes were further studied to analyze the biophysical properties of the protein in the lipid-bound state (see below).

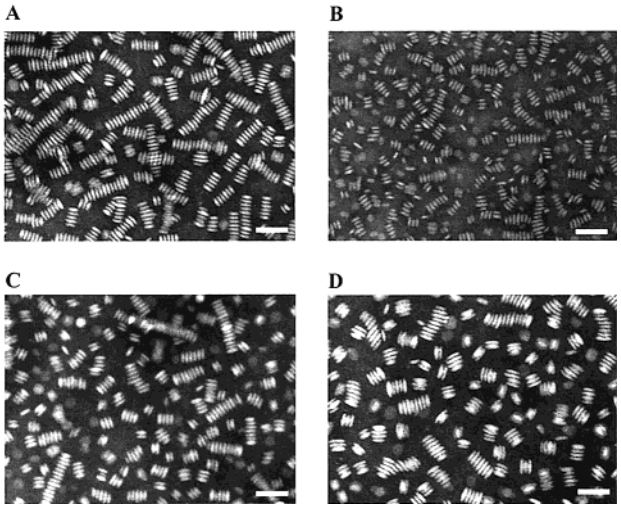

FIGURE 3: Electron micrographs of DMPC/apoLp-III complexes. DMPC vesicles were incubated with apoLp-III and the resulting discoidal complexes were isolated by KBr density gradient ultracentrifugation. Shown are DMPC/apoLp-III discoidal complexes formed with wild-type apoLp-III (panel A), apoLp-III(H1−3) (panel B), apoLp-III(H2−4) (panel C), or apoLp-III(H3−5) (panel D). Samples were negatively stained with 2% phosphotungstate. Bars indicates 50 nm.

Analysis of DMPC/ApoLp-III Complexes. The size of DMPC/apoLp-III complexes differed considerably among the truncation mutants (Table 2). Complexes formed with apoLp-III(H3−5) were significantly larger (diameter 24.8 nm) than the complexes of apoLp-III(H1−3) described earlier (*20*) (Figure 3). Native PAGE analysis revealed complex sizes of about 700 kDa for wild-type apoLp-III and apoLp-III(H2−4)/DMPC disks, 400 kDa for apoLp-III(H1−3), and an

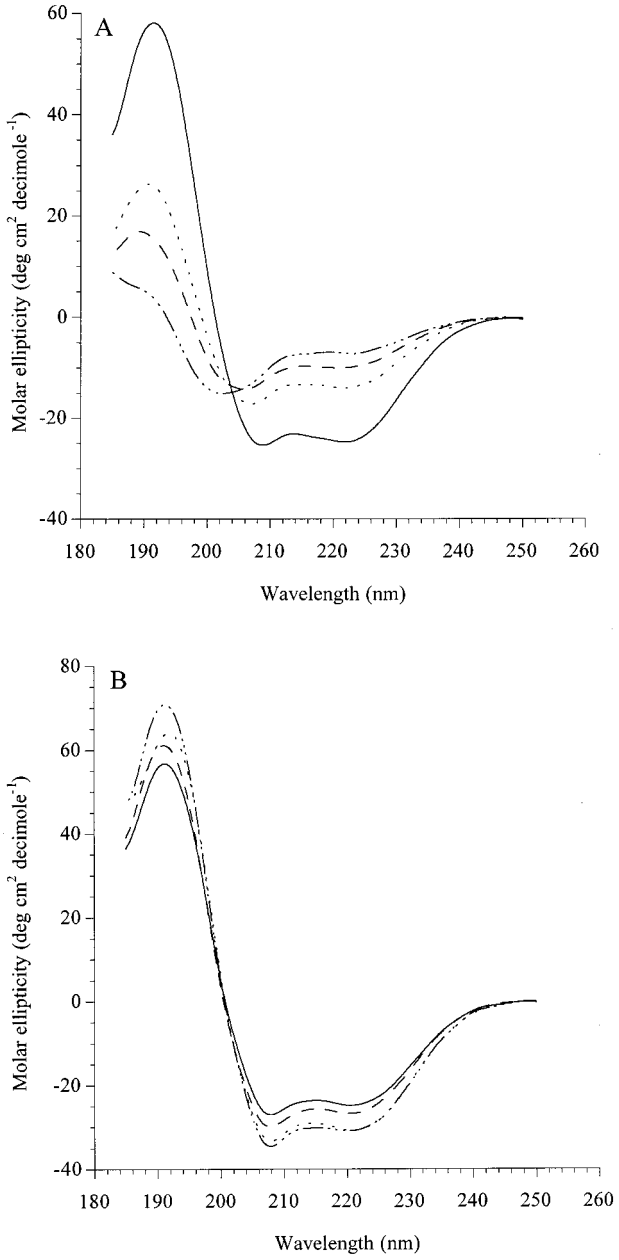

FIGURE 4: Far UV CD spectra of wild-type and truncation mutants of apoLp-III. Panel A: CD spectra in the absence of TFE. Panel B: CD spectra of apoLp-III in the presence of 50% TFE. Spectra were recorded in 50 mM sodium phosphate (pH 7.2). Wild-type apoLp-III (—), apoLp-III(H1−3) (- - -), apoLp-III(H2−4) (— — — —) or apoLp-III(H3−5) (— - - - —).

estimated 900 kDa for apoLp-III(H3−5), in good agreement with the electron microscopic analysis (Table 2).

To determine the number of apoLp-III molecules bound per disk, apoLp-III/DMPC complexes were subjected to chemical cross-linking with dimethyl suberimidate. SDS−PAGE analysis showed that a maximum of six apoLp-III(H2−4) molecules were bound to the DMPC disk (results not shown), compared to five wild-type apoLp-III and seven apoLp-III(H1−3), as reported previously (*20*). However, the large complexes generated with apoLp-III(H3−5) contained nine apoLp-III molecules per DMPC disk.

Biophysical Studies. Far UV CD spectra (Figure 4A) showed that, compared to the highly α-helical wild-type protein, the truncation mutants have considerably less

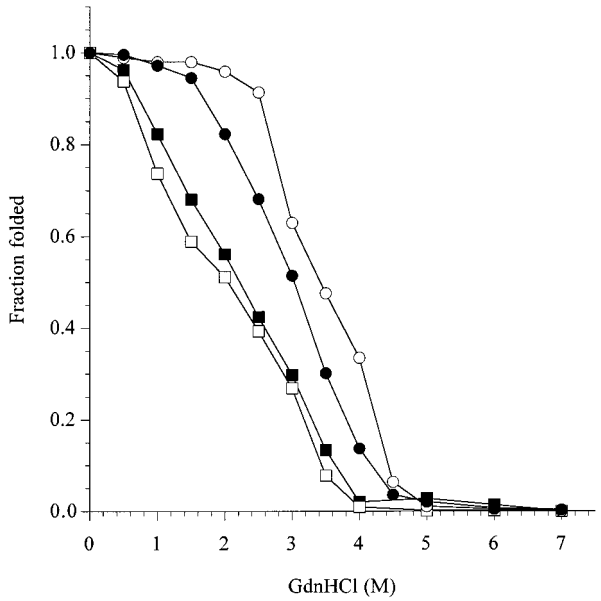

FIGURE 5: Denaturation of DMPC/apoLp-III complexes with guanidine HCl. Complexes were incubated for 24 h with different concentrations of guanidine HCl, and the extent of denaturation was monitored by CD: wild-type apoLp-III (open circles), apoLp-III(H1−3) (closed circles), apoLp-III(H2−4) (closed squares), and apoLp-III(H3−5) (open squares).

secondary structure (Table 1). However, addition of the helix-inducing agent TFE (50%) increased the amount of α-helix to 90−100% for all mutants. In addition, binding to DMPC caused an increase in α-helix content for all proteins to ∼100% (Figure 4B, Table 1). The effect of guanidine HCl exposure on the secondary structure of wild-type apoLp-III and the truncation mutants is shown in Figure 5. Wild-type *G. mellonella* apoLp-III has a denaturation midpoint of 0.3 M, while the corresponding value for apoLp-III(H1−3) was 0.4 M (*20*). Denaturation midpoints for lipid-free apoLp-III(H2−4) and apoLp-III(H3−5) were not determined because the low secondary structure content in buffer prevented accurate measurement. Association with DMPC stabilized the truncation mutants, as shown by their increased resistance to guanidine HCl-induced denaturation. However, apoLp-III(H2−4) and apoLp-III(H3−5) displayed less stability than apoLp-III(H1−3) or wild-type apoLp-III.

Sedimentation equilibrium experiments revealed that the truncation mutants displayed self-association properties in solution, in contrast to full-length apoLp-III, which is monomeric in buffer. Monomers and dimers were found in solutions of all three truncation mutants, while apoLp-III(H2−4) and apoLp-III(H3−5) also showed the presence of small amounts of trimers (Table 1). Chemical cross-linking of solutions of truncation mutants with dimethyl suberimidate and analysis by SDS−PAGE led to similar results (data not shown).

ANS fluorescence was used to evaluate the effect of truncation on relative exposure of hydrophobic sites in apoLp-III. ANS binding to hydrophobic cavities in apoLp-III results in a blue-shift in emission λmax and an increase in ANS fluorescence intensity (*32*). Addition of ANS to apoLp-III solutions showed low ANS fluorescence for all proteins, while emission intensity was lowest for the C-terminal fragment (H3−5) (Figure 6). Previous studies showed that lowering the solution pH induces flexibility in

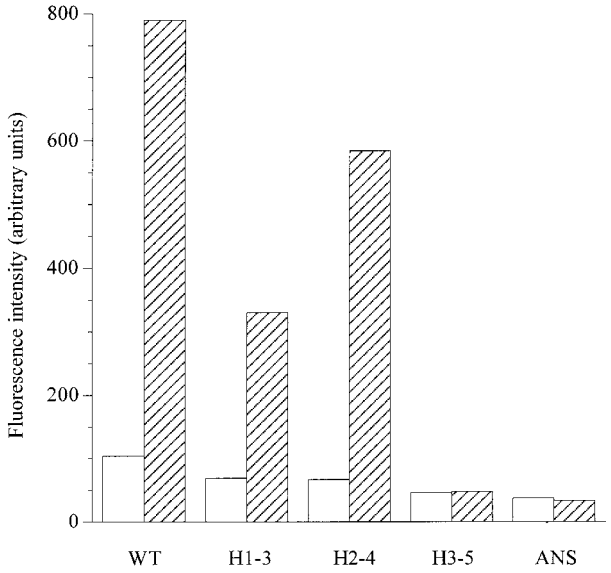

FIGURE 6: Effect of apoLp-III on ANS fluorescence intensity. Apolipoprotein was incubated in the presence of ANS and binding was detected by an increase in ANS fluorescence. The samples were excited at 395 nm, and emission was measured at $\lambda = 470$ nm at pH 7 (white bars) and pH 3 (hatched bars).

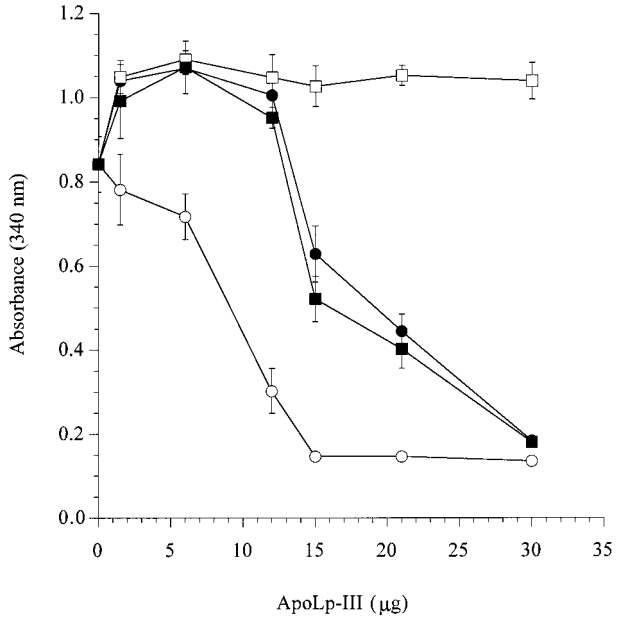

FIGURE 7: Effect of apoLp-III on PL-C-induced LDL aggregation. LDL samples (50 μg protein) were incubated with PL-C (160 mU) in the presence of increasing amounts of apoLp-III. Wild-type apoLp-III binds to PL-C-treated LDL thereby protecting LDL from aggregation, which is evident by the lack of sample turbidity. In the absence of apolipoprotein sample turbidity develops caused by the aggregation of LDL particles. Sample absorbance was determined at 340 nm. Error bars represent the standard deviation of three determinations; wild-type apoLp-III (open circles), apoLp-III(H1−3) (closed circles), apoLp-III(H2−4) (closed squares), apoLp-III(H3−5) (open squares).

protein tertiary structure, thereby increasing ANS accessibility to hydrophobic sites in the protein (*32*). To induce exposure of hydrophobic binding sites, apoLp-III was subjected to acidic conditions. At pH 3, ANS fluorescence emission was strongly increased when incubated with wild-type apoLp-III, apoLp-III (H1−3), and apoLp-III(H2−4). However, ANS fluorescence intensity of the C-terminal fragment remained unchanged, indicating a lack of hydrophobic sites.

Protection Against PL-C-Induced LDL Aggregation. The ability of apoLp-III truncation mutants to interact with spherical lipoproteins was studied using human LDL. Normally, LDL does not contain exchangeable apolipoproteins nor does apoLp-III associate with LDL upon incubation. However, modification of the LDL surface with PL-C creates binding sites for exchangeable apolipoproteins. Whereas PL-C-treated LDL forms aggregates, this can be prevented by inclusion of exchangeable apolipoprotein in the assay (*26*). PL-C-induced LDL aggregation is monitored by measuring sample turbidity as solutions of LDL aggregates have a turbid appearance. Using excess apolipoprotein (50 μg), apoLp-III(H2−4) completely prevented PL-C-induced aggregation of 50 μg of LDL protein, as the absorbance at 340 nm remained low. This is similar to apoLp-III(H1−3) that also inhibits LDL aggregation, indicating lipoprotein binding (*20*). In contrast, apoLp-III(H3−5) lacked the ability to prevent PL-C-induced LDL aggregation as indicated by its high absorbance after a 2 h time span. Inclusion of limiting amounts of apoLp-III in the reaction mixture indicated the relative protection these mutant proteins provided. From such dose−response relationships, shown in Figure 7, wild-type apoLp-III was more effective in preventing aggregation than the truncation mutants. The estimated amount of protein sufficient to prevent 50% of the maximum turbidity after a 2 h incubation was 24 μg for apoLp-III(H1−3) and apoLp-III(H2−4), twice the amount of wild-type apoLp-III (12.5 μg). The C-terminal fragment showed no protection at all protein concentrations used.

DISCUSSION

The aim of this study was to investigate the role of specific helical segments in apoLp-III in protein structure and lipid binding. Studies of fragments of apoLp-III may lead to fundamental insights in the interaction of exchangeable apolipoproteins with lipid surfaces and therefore apolipoprotein function. Two three-helix fragments of *G. mellonella* apoLp-III were designed and analyzed for secondary structure content and lipid binding properties, and compared with an N-terminal fragment characterized recently (*20*). Each truncation mutant encompassed three consecutive helices of the five-helix bundle apolipoprotein creating an N-terminal fragment (H1−3), a core fragment (H2−4), and a C-terminal fragment (H3−5) as depicted in Figure 1. It was hypothesized that these 3-helix proteins may be able to maintain interhelical contacts allowing hydrophobic interactions between nonpolar residues. This would stabilize the native protein structure as interchain interactions are essential for the folding and stability of the 3D structure (*33*). Lack of interhelical contacts may explain the lack of secondary structure and lipid-binding of a peptide fragment encompassing helix five of *M. sexta* apoLp-III (*34*, *35*). In another study, proteolytic cleavage in the center of *L. migratoria* apoLp-III generated two fragments, approximately 2.5 helices long. These fragments also lacked the ability to interact with lipoprotein surfaces (*36*). In contrast to these findings, a 3-helix N-terminal fragment of *G. mellonella* apoLp-III rendered a functional protein (*20*). It is of interest to note that recently a nativelike 3-helix bundle protein was designed de novo (*37*). While it is possible that apoLp-III fragments smaller than three helices bind to lipid, the concept of 3-helix

apolipoproteins with potential for interhelical contacts that stabilize the protein structure in solution may allow identification of specific lipid binding domains in this model apolipoprotein.

The truncation mutants were similar in size as well as in distribution of hydrophobic and charged residues within their primary structure. Also, differences in the hydrophobic moment between the individual helices were small (*20*). Garnier-Osguthorpe-Robson (GOR) secondary structure calculation (*38*) predicted α-helical contents of 86% for wild-type apoLp-III, 81% for apoLp-III(H1−3), 78% for apoLp-III(H2−4), and 87% for apoLp-III(H3−5). However, CD analysis showed that each mutant contained considerably less structure in solution than predicted. The helical content of the core and C-terminal fragments was reduced to ∼25%, while the N-terminal fragment possessed ∼50% α-helix content. Apparently the removal of helices came at a cost, suggesting that all five helices are required to maintain optimal structural integrity of the protein. A decrease in helical content was also observed in studies using synthetic peptides of human apoA-I (*39*). The intrinsic propensity to adopt a highly α-helical structure was not lost as TFE induced the truncation mutants to increase their α-helical content to values similar to wild-type protein. In contrast to wild-type apoLp-III, which is present as a monomer, all truncation mutants demonstrated self-association properties. This might be due to a less ordered structure, and the need for intermolecular contacts to stabilize the protein structure. While apoLp-III(H2−4) and apoLp-III(H3−5) contained little well-defined structure, their lipid surface seeking properties were maintained as the 3-helix mutants were able to associate spontaneously with DMPC vesicles. Association with DMPC led to an increase in α-helical structure, reaching a value similar to that of wild-type apoLp-III complexed with DMPC. ApoLp-III/DMPC complexes also demonstrated increased resistance to guanidine−HCl denaturation, suggesting that the truncated proteins form stable amphipathic α-helices in a membrane environment.

The size of the newly formed lipid−protein complexes differed considerably between the truncation mutants. While apoLp-III(H2−4) formed complexes with a size similar to wild-type apoLp-III-DMPC disks (diameter of ∼18 nm), complexes formed by N-terminal apoLp-III(H1−3) were smaller (∼14 nm) and complexes formed by C-terminal apoLp-III(H3−5) were larger (∼25 nm). The larger disks contained a higher number of apoLp-III molecules, which serve to shield the increased hydrophobic surface on the periphery of the discoidal complexes from the aqueous milieu. The rate of transformation of DMPC bilayer vesicles into DMPC-apoLp-III disk complexes was highest for apoLp-III(H1−3), with a 5-fold slower rate observed for apoLp-III(H3−5). Thus, the smallest complexes were formed with the highest rates, while large complexes were formed at a relatively low transformation rate. In addition, N-terminal and core fragments displayed 5-fold higher transformation rates compared to wild-type apoLp-III. While the smaller size of the fragments could lead to increased diffusion rates and may be partly responsible for the enhanced lipid binding, it is also known that more loosely folded apolipoproteins display a marked increase in DMPC vesicle transformation rate (*32*, *40*). These studies indicated that decreased tertiary structure may favor interaction with DMPC vesicles and may explain the higher vesicle transformation rates of the N- and core fragments compared to the more structured wild-type protein. This is in good agreement with studies using apoA-I peptides demonstrating a much faster rate of phospholipid vesicle clearance compared to full length apoA-I, indicative of a conformational change of intact apoA-I during lipid binding (*39*, *41*).

Despite significant loss of secondary structure, apoLp-III(H1−3) and apoLp-III(H2−4) were able to protect lipolyzed LDL from aggregation. Protection of PL-C-treated LDL is obtained through binding of the apolipoproteins with the modified lipoprotein surface (*26*, *27*). However, the C-terminal fragment failed to protect LDL against PLC-induced aggregation, indicating the absence of lipoprotein binding. Also, no ANS binding was detected in the C-terminal fragment at pH 7 or pH 3, indicating lack of exposed hydrophobic sites. This lack of ANS binding may explain the lack of lipoprotein binding. Although all three fragments have the propensity to bind to lipid bilayers and increase their helicity, lipoprotein binding may require structural elements not present in the C-terminal fragment. In addition, the C-terminal fragment was able to transform DMPC vesicles but at a significant slower rate compared to the other fragments. Although the amount of α-helix in apoLp-III(H2−4) and apoLp-III(H3−5) is equally low (∼25%), the core fragment exhibited lipoprotein binding activity. Thus, secondary structure content only may not explain the observed differences between the truncation mutants. Both apoLp-III(H2−4) and apoLp-III(3−5) contain the sequence that corresponds to the small helix-3′ reported for *M. sexta*-apoLp-III (*4*). Helix-3′ is thought to be involved in lipid surface recognition during lipoprotein binding (*10*). However, helix-3′ appears not to be involved in lipid and lipoprotein binding of the truncated mutants. Perhaps due to structural changes induced by deletions, domains that have the potential to initiate lipid binding, but are buried in the helix bundle fold of the wild-type protein, could become exposed and are available to initiate lipid binding. As apoLp-III(H3−5) is not able to interact with a lipoprotein surface, this is consistent with an earlier observation that helix-5 of *M. sexta* apoLp-III lacked lipoprotein binding activity (*34*).

Taken together, 3-helix apolipoproteins generated from full-length apoLp-III displayed low secondary structure content but were able to adopt the high α-helical content characteristic of exchangeable apolipoproteins by complexation with DMPC or addition of TFE. The lipid binding properties of the three truncation mutants based on both DMPC vesicle clearance data and lipoprotein binding puts them in the following order of lipid binding affinity: helix 1−3 > helix 2−4 > helix 3−5. These results suggest that the structural elements necessary for lipoprotein interaction are located in the N-terminal part of apoLp-III. Also, the 3-helix bundle protein is able to function as a normal apoLp-III, questioning the necessity for five helices in the wild-type protein. However, this may reflect the need of a 5-helix bundle protein for optimized function in lipid binding processes, as well as in unknown specific processes that require the presence of individual helices. They may function in the process of apoLp-III dissociation from lipoprotein surface as a function of lipid removal from the particle (*42*). The construction of the 3-helix mutants has created several opportunities for future research. The smaller protein size

decreases complexity of discoidal complexes and may facilitate NMR studies of apoLp-III in the lipid-bound state. It also benefits physiological studies of apoLp-III, i.e., the role in diacylglycerol transport in vivo and the possible interaction of apoLp-III with fat body lipophorin binding sites (*43*) and in programmed cell death (*44*). Recent studies underline the role of apoLp-III in insect immunity. There is an increasing amount of evidence that apoLp-III undergoes lipid association prior to activation of the immune system. Substitution of Lys68 by Glu resulted in decreased lipoprotein binding and reduced immune activation (*19*); thus disturbance of apoLp-III lipid association in the N-terminal part of the protein affected its immune activation. A subpopulation of immune competent hemocytes of *G. mellonella* specifically takes up an apoLp-III/lipophorin complex, followed by superoxide radical formation (*45*). A receptor responsible for this activation remains to be identified. With the availability of the three-helix truncation mutants, the involvement of different domains in the protein in immune activating processes can be studied in more detail, and the presence of a receptor-competent conformation of apoLp-III that interacts with binding sites on hemocytes (*18*, *19*). Specific sites in the protein involved in these processes can now be targeted in future research.

ACKNOWLEDGMENT

The authors thank Leslie D. Hicks for performing analytical ultracentrifugation experiments, and Roger Bradley for electron microscopy.

REFERENCES

1. Narayanaswami, V., and Ryan, R. O. (2000) *Biochim. Biophys. Acta 1483*, 15−36.
2. Segrest, J. P., Garber, D. W., Brouillette, C. G., Harvey, S. C., and Anantharamaiah, G. M. (1994) *Adv. Protein Chem. 45*, 303−369.
3. Breiter, D. R., Kanost, M. R., Benning, M. M., Wesenberg, G., Law, J. H., Wells, M. A., Rayment, I., and Holden, H. M. (1991) *Biochemistry 30*, 603−608.
4. Wang, J., Gagné, S. M., Sykes, B. D., and Ryan, R. O. (1997) *J. Biol. Chem. 272*, 17912−17920.
5. Wilson, C., Wardell, M. R., Weisgraber, K. H., Mahley, R. W., Agard, D. A. (1991) *Science 252*, 1817−1822.
6. Wientzek, M., Kay, C. M., Oikawa, K., and Ryan, R. O. (1994) *J. Biol. Chem. 269*, 4601−4612.
7. Weers, P. M. M., Wientzek, M., Kay, C. M., and Ryan, R. O. (1994) *Biochemistry 33*, 3617−3624.
8. Raussens, V., Narayanaswami, V., Goormaghtigh, E., Ryan, R. O., and Ruysschaert, J.-M. (1995) *J. Biol. Chem. 270*, 12542−12547.
9. Narayanaswami, V., Wang, J., Schieve, D., Kay, C. M., Scraba, D. G., and Ryan, R. O. (1996) *J. Biol. Chem. 271*, 26855−26862.
10. Narayanaswami, V., Wang, J., Schieve, D., Kay, C. M., and Ryan, R. O. (1999) *Proc. Natl. Acad. Sci. U.S.A. 96*, 4366−4371.
11. Weers, P. M. M., Narayanaswami, V., Kay, C. M., and Ryan, R. O. (1999) *J. Biol. Chem. 274*, 21894−21810.
12. Soulages, J. L., and Arrese, E. L. (2000) *J. Biol. Chem. 275*, 17501−17509.
13. Soulages, J. L., Arrese, E. L., Chetty, P. S., and Rodriquez, V. (2001) *J. Biol. Chem. 276*, 34162−34166.
14. Ryan, R. O., and Van der Horst D. J. (2000) *Annu. Rev. Entomol. 45*, 231−258.
15. Soulages, J. L., and Wells M. A. (1994) *Adv. Protein Chem. 45*, 371−415.
16. Wiesner, A., Losen, S., Kopácek, P., and Götz. P. (1997) *J. Insect Physiol. 43*, 383−391.
17. Niere, M., Meisslitzer, C., Dettloff, M., Weise, C., Ziegler, M., and Wiesner A. (1999) *Biochim. Biophys. Acta 1433*, 16−26.
18. Dettloff, M., Kaiser, B., and Wiesner, A. (2001) *J. Insect Physiol. 47*, 789−797.
19. Niere, M., Dettloff, M., Maier, T., Ziegler, M., and Wiesner, A. (2001) *Biochemistry 40*, 11502−11508.
20. Dettloff, M., Weers, P. M. M., Niere, M., Kay, C. M., Ryan, R. O., and Wiesner, A. (2001) *Biochemistry 40*, 3150−3157.
21. Laemmli, U. K. (1970) *Nature 227*, 680−685.
22. Provencher, S. W., and Glöckner, J. (1981) *Biochemistry 20*, 33−37.
23. Laue, T. M., and Stafford, W. F., III. (1999) *Annu. Rev. Biophys. Biomol. Struct. 28*, 75−100.
24. Johnson, M. L., Correia, J. J., Yphantis, D. A., and Halvorson, H. R. (1981) *Biophys. J. 36*, 575−588.
25. Laue, T. M., Shah, B. D., Ridgeway, T. M., and Pelletier, S. L. (1991) in *Analytical Ultracentrifugation in Biochemistry and Polymer Science* (Harding, S. E., Rowe, A. J., and Horton, J. C., Eds.) pp 90−125, Royal Society of Chemistry, Cambridge, UK.
26. Liu, H., Scraba, D. G., and Ryan R. O. (1993) *FEBS Lett. 316*, 27−33.
27. Weers, P. M. M., Van der Horst, D. J., and Ryan, R. O. (2000) *J. Lipid Res. 41*, 416−423.
28. Weise, C., Franke, P., Kopacek, P., and Wiesner, A. (1998) *J. Protein Chem. 17*, 633−641.
29. Ryan, R. O., Schieve, D., Wientzek, M., Narayanaswami, V., Oikawa, K., Kay, C. M., and Agellon, L. B. (1994) *J. Lipid Res. 36*, 1066−1072.
30. Fisher, C. A., Wang, J., Francis, G. A., Sykes, B. D., Kay, C. M., and Ryan, R. O. (1997) *Biochem. Cell Biol. 75*, 45−53.
31. Weers, P. M. M., Wang, J., Kay, C. M., Van de Horst, D. J., and Ryan, R. O. (1998) *Biochim. Biophys. Acta 1393*, 99−107.
32. Weers, P. M. M., Kay, C. M., and Ryan, R. O. (2001) *Biochemistry 40*, 7754−7760.
33. Mant, C. T., Zhou, N. E., and Hodges, R. S. (1993) in *The Amphipathic* (Helix, and Epand, R. M., Eds.) pp 39−64, CRC Press Inc., Boca Raton, FL.
34. Narayanaswami, V., Kay, C. M., Oikawa, K., and Ryan, R. O. (1994) *Biochemistry 33*, 13312−13320.
35. Wang, J., Narayanaswami, V., Sykes, B. D., and Ryan, R. O. (1998) *Protein Sci. 7*, 336−341.
36. Narayanaswami, V., Weers, P. M. M., Bogerd, J., Kooiman, F. P., Kay, C. M., Scraba, D. G., Van der Horst, D. J., and Ryan, R. O. (1995) *Biochemistry 34*, 11822−11830.
37. Walsh, S. T. R., Cheng, H., Bryson, J. W., Roder, H., and DeGrado, W. F. (1999) *Proc. Natl. Acad. Sci. U.S.A. 96*, 5486-5491.
38. Garnier, J., Gibrat, J. F., and Robson., B. (1996) *Methods Enzymol. 266*, 540−553.
39. Palgunachari, M. N., Mishra, V. K., Lund-Katz, S., Phillips, M. C., Adeyeye, S. O., Alluri, S., Anantharamaiah, G. M., and Segrest, J. P. (1996) *Arterioscler. Thromb. Vasc. Biol. 16*, 328−338.
40. Soulages, J. L., and Bendavid, O. J. (1998) *Biochemistry 37*, 10203−10210.
41. Mishra, V. K., Palgunachari, M. N., Datta, G., Phillips, M. C., Lund-Katz, S., Adeyeye, S. O., Segrest, J. P., and Anantharamaiah, G. M. (1998) *Biochemistry 37*, 10313−10324.
42. Van der Horst, D. J. (1990) *Biochim. Biophys. Acta 1047*, 195−211.
43. Dantuma, N. P., Potters, M., De Winther, M. P. J., Tensen, C. P., Kooiman, F. P., Bogerd, J., and Van der Horst, D. J. (1999) *J. Lipid Res. 40*, 973−978.
44. Sun, D., Ziegler, R., Milligan, C. E., Fahrbach, S., and Schwartz, L. M. (1995) *J. Neurobiol. 26*, 119−129.
45. Dettloff, M., Wittwer, D., Weise, C., and Wiesner, A. (2001) *Cell Tissue Res. 306*, 449−458.

BI0200108